Available online at www.sciencedirect.com

SCIENCE DIRECT®

International Journal of Coal Geology 66 (2006) 119–136

International Journal of COAL GEOLOGY

www.elsevier.com/locate/ijcoalgeo

Geochemistry and mineralogy of the Cretaceous Wulantuga high-germanium coal deposit in Shengli coal field, Inner Mongolia, Northeastern China

Xinguo Zhuang [a], Xavier Querol [b,*], Andrés Alastuey [b], Roberto Juan [c], Felicià Plana [b], Angel Lopez-Soler [b], Guang Du [d], Victor V. Martynov [e]

[a] *Institute of Basin Analysis, China University of Geosciences, Wuhan, 430074, People's Republic of China*
[b] *Institute of Earth Science 'Jaume Almera' CSIC, C/LLuis Solé y Sabarís s/n, 08028 Barcelona, Spain*
[c] *Institute of Coal Chemistry, C/ Miguel Luesma Castán, 4, 50018 Zaragoza, Spain*
[d] *Coal Geological Bureau of Inner Mongolia, Huhehot, 010051, People's Republic of China*
[e] *Nuclear Physics Institute Russian Academy of Sciences, Gatchina, Leningrad District 188300, Russia*

Received 8 October 2004; received in revised form 13 June 2005; accepted 21 June 2005
Available online 22 September 2005

Abstract

The occurrence and distribution of minerals, and major and trace elements of the coal #6-1 from the Cretaceous Wulantuga high-germanium coal deposit in Shengli coal field, Inner Mongolia are investigated.

The major mineral constituents of coal #6-1 are quartz (15%), kaolinite (4–5%), illite (1%), pyrite (<1%), feldspars (<1%), gypsum (weathering product, <2%) and traces of chlorite. In addition to these phases, traces of scheelite ($CaWO_4$) and weddellite (an oxalate, $CaC_2O_4 \cdot 2H_2O$) were also detected by XRD. On the basis of chemical and mineralogical properties, a clear differentiation was found between the upper and lower coal sections: the lower section with higher sulfide mineral content, and the upper one with low sulfur content and with a higher proportion of mineral phases formed/accumulated under oxidizing conditions (quartz and dolomite). This coal seam is highly enriched in Ge, As, W, and Hg (one to two orders of magnitude higher than the usual worldwide coal concentrations), with high contents of Sb, U, Cs, and Be (one order of magnitude higher than the usual worldwide coal concentrations). The geochemical and mineralogical profile patterns of the coal seam were attributed to the development of a basal reduced marsh environment evolving towards a more oxidizing marsh environment in the upper part of the coal seam. This could be related to the evolution from a high water table low moor marsh environment to a high moor marsh into an open water body with a higher detrital influence at the top of the seam.

* Corresponding author. Tel.: +34 934095410; fax: +34 934110012.
E-mail address: xavier.querol@ija.csic.es (X. Querol).

0166-5162/$ - see front matter
doi:10.1016/j.coal.2005.06.005

These syngenetic geochemical characteristics are possibly modified by an unusually intensive hydrothermal alteration causing the formation of oxalate minerals and the enrichment in a series of elements such as Cs, Be, U, As, Se, and Hg.

Keywords: Geochemistry; Coal; Metals; Germanium; China; Inner Mongolia

1. Introduction

The Cretaceous high-Ge Wulantuga coal open pit mine is located 13 km to the west of the town of Xilinhaote (Inner Mongolia, Northeastern China, Fig. 1) and was discovered by the Bureau of Coal Geological Exploration of Inner Mongolia in 1998. According to Wang (1999), this coal deposit belongs to the Early Cretaceous Southwestern Shengli coalfield (Fig. 1).

This deposit consists of a monocline structure (with NW slope) limited by two normal faults on the northeastern and southwestern boundaries (Fig. 2). This simple geological structure makes possible open pit mining.

Li et al. (1984, 1988) differentiated three zones for the Mesozoic coal basins in Northeast China from West to East. The study basin is in the first zone of the Early Cretaceous (Fig. 1). This and the second zone (between Chifeng and Shenyang cities) contain the highest number of coal basins and resources, with the best coal quality in Northeastern China. These faulted basins isolated, but their comparable depositional sequences indicate a similar and possibly a synchronous tectonic evolution as reported by Li et al. (1984, 1988) and Querol et al. (1997b). The latter authors found the same facies distribution in many of the faulted basin, with alluvial fan units (with coarse sediments at the bottom) along marginal contemporaneous faults, and with coal deposits in the distal areas.

The main tectonic stages affected northeast China during the Mesozoic (Li et al., 1984, 1988):

1) A compressive stage (Middle Jurassic, Yenshan stage) with intense folding and magmatic intrusions and a dominant northeast trending.
2) Subsequently, large areas of eastern China were uplifted and denudated.
3) From the late Jurassic, taphrogenesis prevailed with three main volcanic cycles (from basic to acidic) following a very deep north-northeast faulting system.
4) At the end of the Late Jurassic, basal clastic deposits and thick lacustrine sediments interlayered with suites of volcanic rocks.

The weakening of the upper layer of the Earth's crust by magmatic episodes and consequent thermal processes provided a suitable framework for the formation and maturation of coal deposits in faulted basins during the Late Jurassic and the Early Cretaceous. Many of these were formed on volcanic basements, and thus the distribution of coal basins is closely connected with volcanic zones. The Shengli coal field was developed after a period of high volcanic activity.

Concerning coal quality the Shengli coal is a medium ash coal, with relatively low sulfur content and a subbituminous rank. The coal production in this coalfield reaches about 1 million Mt (tonne). In this area Ge is being extracted from coal ash, and an area of 0.72 km^2 has been investigated for Ge beneficiation (Fig. 2). The recoverable resources are estimated at 6 Mt of brown coal with a Ge content >30 g/t on a whole coal basis, and 1600 tonnes of metallic Ge extractable from coal with a Ge content >100 g/t (Wang, 1999).

Wu et al. (2002) reported the occurrence of another high Ge-coal deposit in the Yimin coalfield (Early Cretaceous faulted basin, North of Shengli coalfield) with an estimated resource of 4000 tonnes of metallic Ge. Therefore, the Early Cretaceous coal-bearing basins in the first zone of Mesozoic coal basins in northeast China may be regarded as an important germanium-bearing coal deposit.

The main Ge ore in the Shengli coalfield is coal seam #6 in the upper coal-bearing member of the

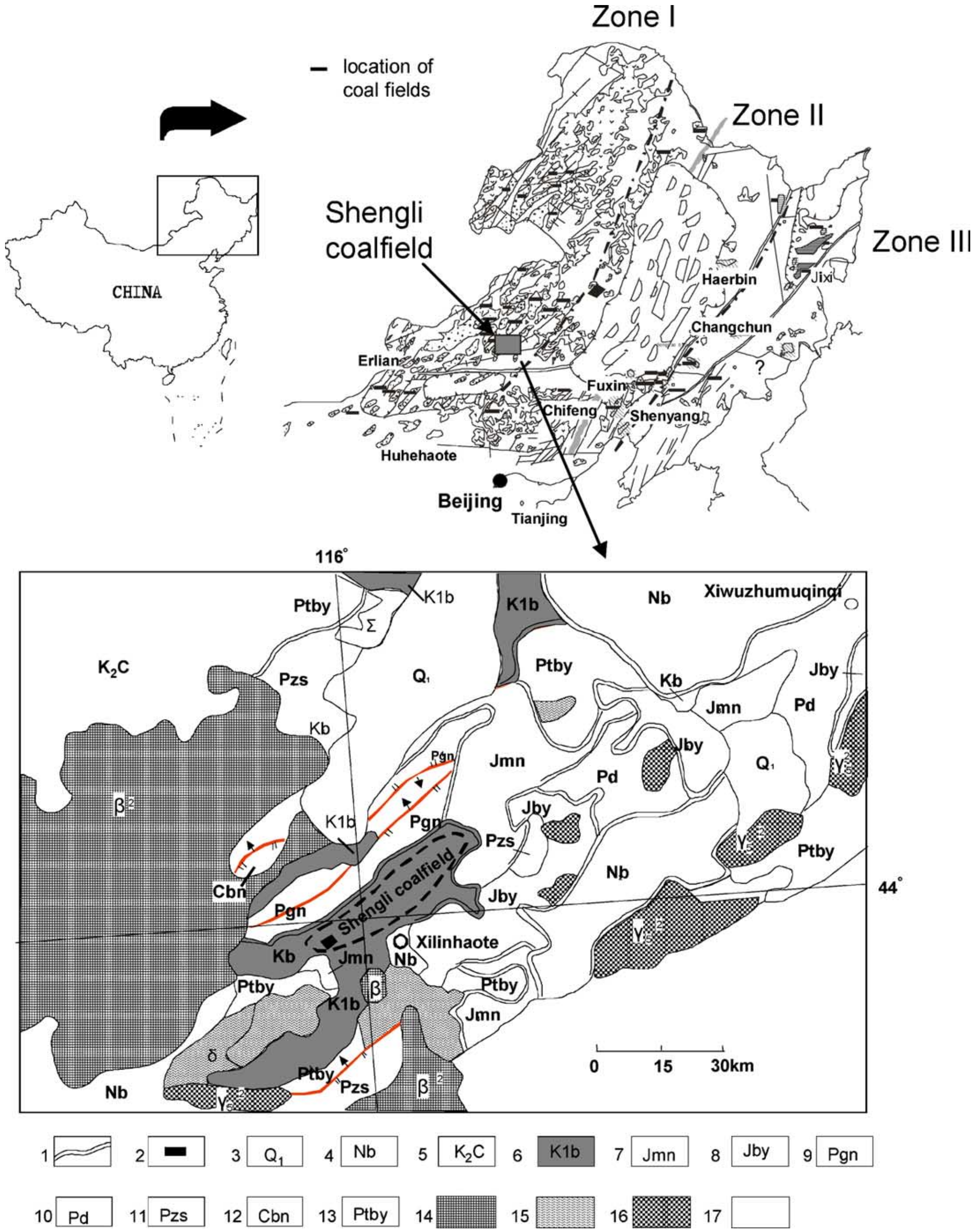

Fig. 1. Geological map of the Wulantuga germanium-coal deposit (after Wang, 1999). 1, unconformity; 2, germanium-bearing coal deposit; 3, Quaternary; 4, Bogedawula formation of Tertiary; 5, Erlian formation of upper Cretaceous; 6, Beiyanhua formation of lower Cretaceous; 7, Manitu formation of upper Jurassic; 8, Beiyingaolao formation of upper Jurassic; 9, Gegenaobao formation of lower Permian; 10, Dashizai formation of lower Permian; 11, Zesi formation of lower Permian; 12, Benbatu formation of upper Carbonifeous; 13, Baoyintu formation of Pt; 14, Quaternary basalt; 15, diorite of Mesozoic; 16, granitic diorite of Mesozoic; 17, granite of the end of late Jurassic; 18.

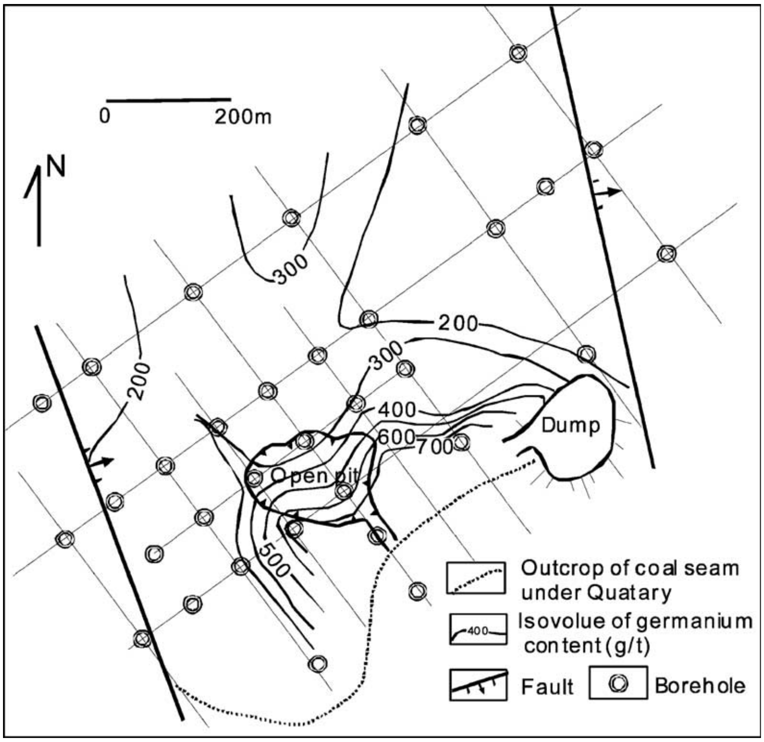

Fig. 2. Distribution of germanium contents (g/t) of the Wulantuga germanium-coal deposit (after Wang, 1999).

Baiyanhua formation (Early Cetaceous). The coal seam #6 is locally split into two seams (6-1 and 6-2) by mudstone and siltstone intercalations with a total thickness of 4–11 m. The overlying unit of this coal seam is made up of mudstone, sandstone and conglomerate, and the underlying unit consists of mudstone and siltstone. The mean thickness of the coal seam #6-1 reaches 9.7 m (range from 0.9 to 17 m). The lower part contains a mudstone parting (0.15–0.30 m). Wang (1999) reported that the Ge content in coal #6-1 ranged from 135 to 820 g/t on a whole coal basis, with a mean of 244 g/t. Coal seam #6-2 is thinner than #6-1, (0−4.9 m), and the Ge content ranges from 10 to 110 g/t, with a mean 27 g/t. The concentrations of Ge in the overlying and underlying clastic rocks are much lower, in the range of 2 to 13 g/t, with a mean 7 g/t. Only the coaly mudstone of seam #6-1 has a relatively high Ge content (17 to 173 g/t, mean 87 g/t).

With the aim of characterizing this peculiar coal, this study focuses on the geochemistry and mineralogy of samples collected from coal seam #6-1 from the Wulantuga germanium-coal deposit.

2. Methodology

Twelve coal channel samples were collected from the coal seam #6-1 from the Wulantuga high Ge-coal open pit mine, using a channel profile sampling strategy. From top to bottom (MY-2 to MY-14, see Table 1), samples 0.3 to 0.9 m thick and 0.25 m wide were collected following a channel sampling profile, depending on macrolithotype, across the whole coal seam (7.5 m thick in this location).

Proximate and ultimate analyses of the coal samples were performed using the following ISO and ASTM recommendations (ISO-589, 1981; ISO-1171, 1976; ISO-562, 1974; ASTM D-3286, 1996).

Mineralogical analyses of the coal samples were performed by means of X-ray diffraction (XRD). Semi-quantitative XRD analysis was performed by using the Reference Internal Standard Method

Table 1
Moisture contents, ash and volatile matter yields, calorific value and contents of C, H, N and S for the channel samples from coal seam #6-1 of the Wulantuga mine in Shengli coal field

	Thickness (m)		Moisture %	Ash db %	V. M. % daf	C % daf	H % daf	N % daf	S % db	CV MJ/kg	CV kcal/kg
MY-2	Top	0.6	18	32	51	65	1.5	0.9	0.2	20.27	4842
MY-3		0.6	22	29	53	65	0.4	2.2	0.3	20.59	4918
MY-4		0.6	17	33	51	66	2.0	1.0	0.3	21.39	5108
MY-5		0.9	21	19	47	70	0.9	1.9	0.3	22.72	5426
MY-6		0.6	21	14	46	71	1.0	1.0	0.3	23.02	5499
MY-7		0.6	19	14	54	66	1.8	1.0	0.5	21.61	5160
MY-8		0.6	16	9	42	76	2.9	0.9	2.0	26.79	6398
MY-9		0.3	18	5	46	72	3.6	0.7	1.5	25.86	6178
MY-10		0.9	19	12	42	75	2.9	0.8	1.8	26.68	6373
MY-11		0.6	18	33	44	73	2.5	0.8	1.7	25.90	6186
MY-12		0.6	22	9	47	75	3.6	0.8	1.1	26.74	6387
MY-14	Bottom	0.6	18	24	47	81	4.1	0.9	3.0	24.64	5885

Vol. M., volatile matter; CV, calorific value; db, dry basis; daf, dry ash free; as rec., as received.

(Chung, 1974). The occurrence of mineral species was also investigated by means of a JEOL 6400 scanning electron microscope (SEM) with a LINK LZ5 EDX analyzer.

Maceral analyses, carried out to investigate coal facies, followed the International Committee for Coal and Organic Petrology (ICCP System 1994) classification and used conventional reflected-light, oil-immersion microscopy. Fluorescent microscopy was used for liptinite maceral analysis.

Coal samples were acid digested following a two-step digestion method devised to retain volatile elements in coal disolution (Querol et al., 1997a). The resulting solutions were analysed by Inductively Coupled Plasma Atomic-Emission Spectrometry (ICP-AES) for major and selected trace elements and by Inductively Coupled Plasma Mass Spectrometry (ICP-MS) for most trace elements. Digestion of international reference materials (SARM-19) and blanks were prepared following the same procedure. Analytical errors were estimated at <3% for most of the elements and around 10% for Cd, Mo, and P.

Hg analyses were performed directly on solid samples using a LECO AMA 254 gold amalgam atomic absorption spectrometer.

Concentration levels of Au and Platinum group elements (PGE) were determined by means of instrumental Neutron Activation Analysis (INAA) at St. Petersburg Nuclear Physics Institute. The irradiation was made during 6 h in the thermal neutron flux of 2.67 E+13 and the epithermal neutron flux of 1.70 E+12. Three measurements of every sample were made after 1, 3 and 10 days.

3. Results and discussion

3.1. Coal characterization

This coal seam is characterized by a relatively high ash yield (21%) and relatively low calorific value (5697 kcal/kg da, equivalent to 23.85 MJ/kg) and sulfur content (1% db). As shown in Table 1, for the coal samples with HTA yield <20%, the moisture (16–22% as received), carbon (66–76% daf) and volatile matter (42–54% daf) contents indicate a subbituminous coalification rank. The volatile matter yields and N contents in the half upper section of the coal seam (MY-2 to MY-7) are higher than those from lower section (MY-8 to MY-14), whereas calorific value, C, H, and S exhibit an opposite profile distribution to N and volatile matter. Consequently, an unusual negative correlation between volatile matter and H contents is found.

3.2. Mineralogy

The major mineral constituents of coal seam #6-1 from the Shengli coal (Table 2) are quartz (15%), kaolinite (4–5%), illite (1%), pyrite (<1%), feldspars (<1%) and traces of clinochlore. Gypsum is a weathering product present in appreciable amounts (<2%).

Table 2
Semi-quantitative mineral composition of channel samples from coal #6-1 from the Wulantuga mine in Shengli coal field as deduced from XRD analysis

Sample	Weddellite	Sheellite	Illite	Kaolinite	Quartz	Chlorite	Dolomite	Pyrite	Gypsum	Feldspar
MY-2	<0.5	<0.5	1.5	2.8	28.1	<0.5	<0.5	<0.5	<0.5	<0.5
MY-3	<0.5	<0.5	0.6	2.0	25.3	<0.5	1.0	<0.5	<0.5	1.0
MY-4	<0.5	<0.5	0.5	3.2	29.7	<0.5	1.0	<0.5	<0.5	<0.5
MY-5	<0.5	<0.5	0.6	6.9	11.0	<0.5	<0.5	<0.5	<0.5	1.0
MY-6	<0.5	<0.5	<0.5	4.8	7.9	<0.5	<0.5	<0.5	<0.5	1.3
MY-7	traces	traces	1.5	0.8	12.8	<0.5	<0.5	<0.5	<0.5	<0.5
MY-8	<0.5	<0.5	traces	6.5	4.2	<0.5	<0.5	1.5	3.4	<0.5
MY-9	<0.5	<0.5	<0.5	<0.5	<0.5	<0.5	<0.5	2.2	2.5	<0.5
MY-10	<0.5	<0.5	traces	3.3	8.9	<0.5	<0.5	1.7	3.1	<0.5
MY-11	<0.5	<0.5	1.8	5.3	26.5	traces	<0.5	<0.5	5.3	<0.5
MY-12	<0.5	<0.5	<0.5	6.8	2.3	traces	<0.5	1.0	1.5	<0.5
MY-14	<0.5	<0.5	2.0	8.6	7.0	traces	<0.5	4.5	6.7	<0.5

Rarely, traces of scheelite ($CaWO_4$) and weddellite (an oxalate, $CaC_2O_4 \cdot 2H_2O$) were also detected by XRD (Fig. 3). Scheelite has probably a detrital origin from intrusive and volcanic rocks and it was detected as a trace component by XRD analysis in the HTA samples containing high W contents. Weddellite is a Ca salt of oxalic acid ($H_2C_2O_4$). The calcium in weddellite replaces the hydrogen in the oxalic acid by reacting with calcium hydroxide or calcite. This reaction produces molecules of mono-hydrated calcium oxalate (whewellite) and water. The source of the oxalic acid is undoubtedly organic and can come from coal or organic debris in sedimentary rocks. This mineral has been found in some coal deposits, such as the Chai-Tumus or Tayllakh brown coal deposits (Siberia, http://www.mindat.org/min-4254.html) or the Holocene Philippi peat in Greece (Kalaitzidis and Christanis, 2002), and in sedimentary mineralizations. However, it has been also found in some hydrothermal veins. When present in coal deposits, this mineral is usually associated with other Na, Mg, Fe or Cu oxalates (http://www.mindat.org/min-4254.html). Kalaitzidis and Christanis (2002) found this mineral in a high As, Se, Br, and U peat deposit. Consequently, this mineral may be of syngenetic or epigenetic origin or related to weathering processes.

The top 2 m of the coal seam shows very high quartz content (25–30%). In the rest of the seam this is considerably reduced (from <1% to 13%), with exception of MY-11 (26%). Feldspars and dolomite are also detected by XRD in the top 2 m of the coal seam (<1%). On the other hand, the lower section of the coal seam (from MY-8 to 14) is enriched in pyrite (1–5%, with exception of MY-11, <0.5%) and gypsum 1–7%.

It is important to note that this coal has a very high Ca content (see the high anhydrite content in the HTA originated by reaction of SO_2 with CaO during combustion, Fig. 3) but calcite was not detected by XRD analysis, suggesting a major organic affinity for this element.

In accordance with the mineralogy described, the coal seam is characterized by an upper 2 m section with a high detrital input of quartz, with minor amounts of clay minerals, feldspars and dolomite (MY2-4). The central section (MY-5-MY10) is characterized by lower quartz detrital quartz influx, a similar clay mineral occurrence and a relatively higher content of pyrite (mostly syngenetic as deduced from microscopical observations), the later probably caused by a more reducing environment. The lower section (MY-11-MY14) contains a similar mineral paragenesis to the middle section, with slightly higher clay mineral content.

SEM observations, coupled with EDX analysis, confirmed the presence of Ge in coal samples MY7 and MY9. Germanium was observed in very small and thin particles (diameter <0.5 μm) generally associated to organic particles (Fig. 4 top). Occasionally, the Ge phases have been identified together with the presence of Au (Fig. 4, top right). SEM observation of coal ash samples also enabled us to identify the common occurrence of small particles (<1 μm) consisting of W and Ca, with traces of Fe, Si, S, and Ge

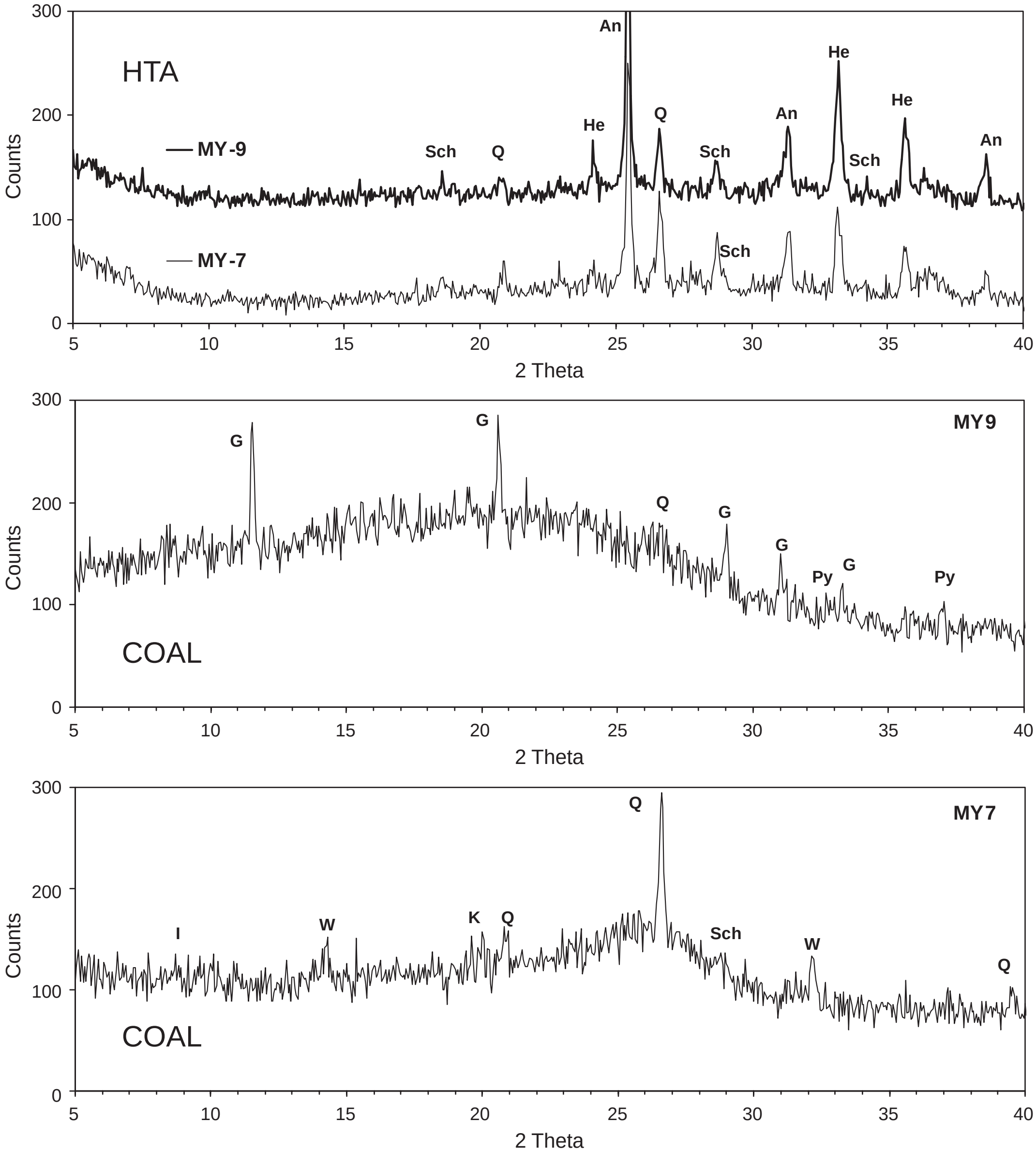

Fig. 3. XRD patterns of MY7 and MY9 bulk coal and HTA samples. W, weddellite; Q, quartz; K, kaolinite; I, illite, Sch, scheelite; G, gypsum, Py pyrite, An, anhydrite, He hematite.

(ash samples MY7 and MY9, Fig. 4 bottom), probably attributable to the presence of very fine scheellite grains as identified by XRD analysis. The occurrence of weddellite was also confirmed by the occurrence of high Ca particles detected by SEM analysis (Fig. 5) as dispersed grains with a wide size range in the samples were this phase was identified by XRD.

3.3. Coal petrology

Table 3 shows quantitative data on maceral content of selected samples from coal seam #6-1 from Wulantuga mine in Shengli coal field. The results show a high vitrinite (54–98%), low to medium inertinite (<1–30%) and liptinite (2–17.5%) con-

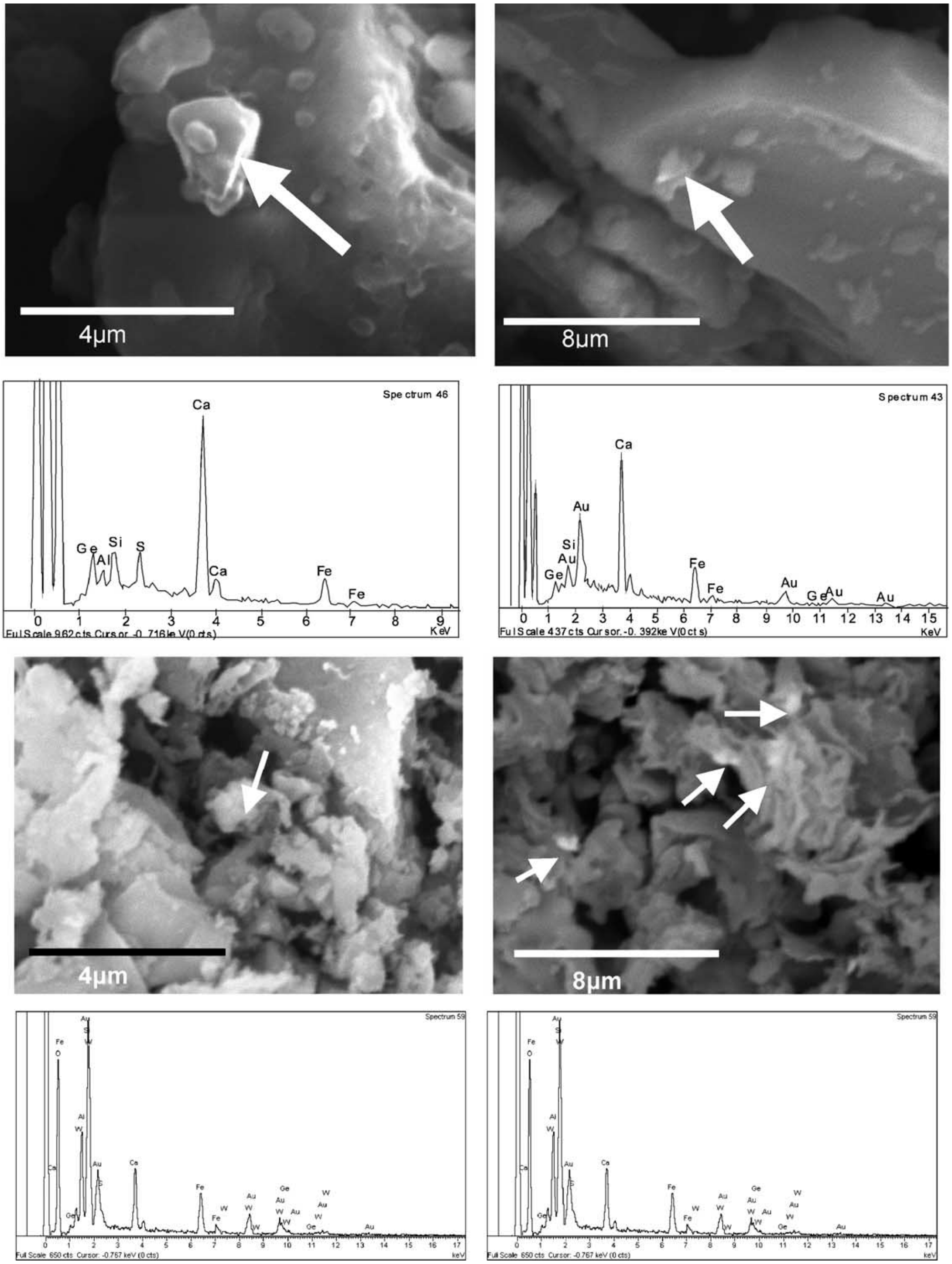

Fig. 4. SEM microphotographies and EDAX spectra: top left, coal sample MY9, small and thin plate particle of Ge oxides (sample not coated with Au); top right, coal sample MY7: Ge oxides with traces of Au, (sample not coated with Au); bottom left and right, particles consisting of W, Ca, and traces of Fe, Si, S, and Ge (samples coated with Au).

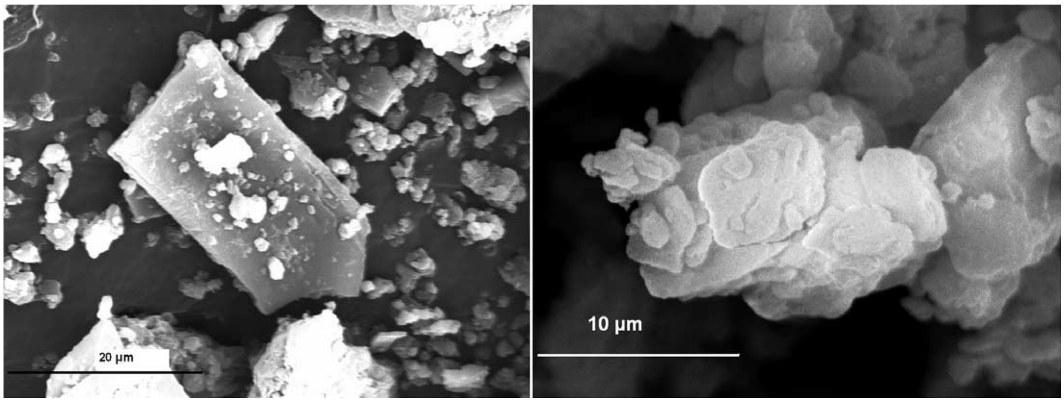

Fig. 5. SEM microphotographies of Ca oxalate grains (laminar grains in both images) in sample MY-7 (samples coated with Au).

tents. The major macerals of the vitrinite group are telinite, desmocollinite, and vitrodetrinite (Fig. 6). The dominant macerals of the inertinite group are semifusinite and fusinite (Fig. 7); whereas for the liptinite group, liptodetrinite, cutinite, sporinite, and resinite predominate. It is clearly evidenced that the bottom (MY-14) and the middle (MY-7, MY-8) sections of the coal seam have higher inertinite (25–30%) and lower vitrinite (54–65%) contents with respect to the middle-low section (MY-9, MY-12), with low inertinite content (<1%) and ash yields (5% and 9%) and a very high vitrinite content (81–98%). In these samples the contents of liptinite vary widely, the liptinite contents of MY-14, MY-7, and MY-8 are 11%, 10% and 16% respectively, and the of MY-9 and MY-12 are 2% and 18% respectively. The inertinite (8–11%), liptinite (7.5–9.8%) and vitrinite (79–85%) contents of the top samples (MY2, MY3) are intermediate. Pyrite is present mainly as massive cell filling mineralizations in telinite, fusinite, and semifusinite in the bottom section (MY-14), and in framboidal aggregates in the middle section (MY-8) (Fig. 8). The occurrence of pyrite in the top section is very rare.

Table 3
Maceral analysis of the selected samples from coal seam #6-1 from the Wulantuga mine in Shengli coal field

	Tel	Teloc	Corp	Desm	Vd	Fus	Semifus	Id	Liptinite
MY-2	21.0	1.9	<0.1	26.5	35.1	2.3	4.5	1.4	7.5
My-3	27.4	4.4	<0.1	34.1	13.1	1.7	9.5	<0.1	9.8
MY-7	32.1	9.8	<0.1	15.3	8.1	12.6	10.8	1.6	9.7
MY-8	24.0	0.4	0.4	18.3	11.0	7.2	21.0	1.9	15.8
MY-9	7.9	3.3	<0.1	67.7	19.1	<0.1	<0.1	<0.1	2.0
MY12	39.8	<0.1	7.5	20.5	13.8	0.8	<0.1	<0.1	17.5
MY-14	28.6	1.4	<0.1	22.7	8.0	5.1	23.4	<0.1	10.7

Tel, Telinite; Teloc, Telocollinite; Corp, Corpcollinite: Desm, Desmocollinite; Vd, Vitrodetrinite; Fus, Fusinite; Semifus, Semifusinite; Id, Inertodetrinite.

According to the maceral composition of the studied coal samples and the studies of Gruber and Sachsenhofer (2001), Bechtel et al. (2003, 2004), the evolution of the type of coal facies in the studied coal seam might be summarized as follows:

The high inertinite (29%) and ash (24%) contents of the bottom coal section (MY-14) suggest an oxidizing raised marsh environment with a higher detrital influence. The pyrite in the coal formed mainly in the diagenetic stage.

The high vitrinite (81–98%) and very low inertinite (<1%) and ash (5–9%) contents measured in the middle-low section of the coal seam (MY-9 and 12) suggest a high water table stage with a prevalent reducing low-lying marsh with a lower detrital influence. The relatively high telinite (40%), corpcollinite (7.5%) and liptinite (17.5%) contents in MY-12, and the high desmocollinite (68%), vitrodetrinite (19%) and low liptinite (2%) contents in MY-9 suggest likely that the accumulated depositional velocity of the peat decreased from MY-12 to MY-9 and the flora change from the forest swamp in MY-12 to the reed marsh in MY-9.

The high inertinite (25–30%) and low-middle ash (9–14%) contents measured for the middle section of the coal seam (MY-7 and 8) suggests an oxidizing raised marsh environment.

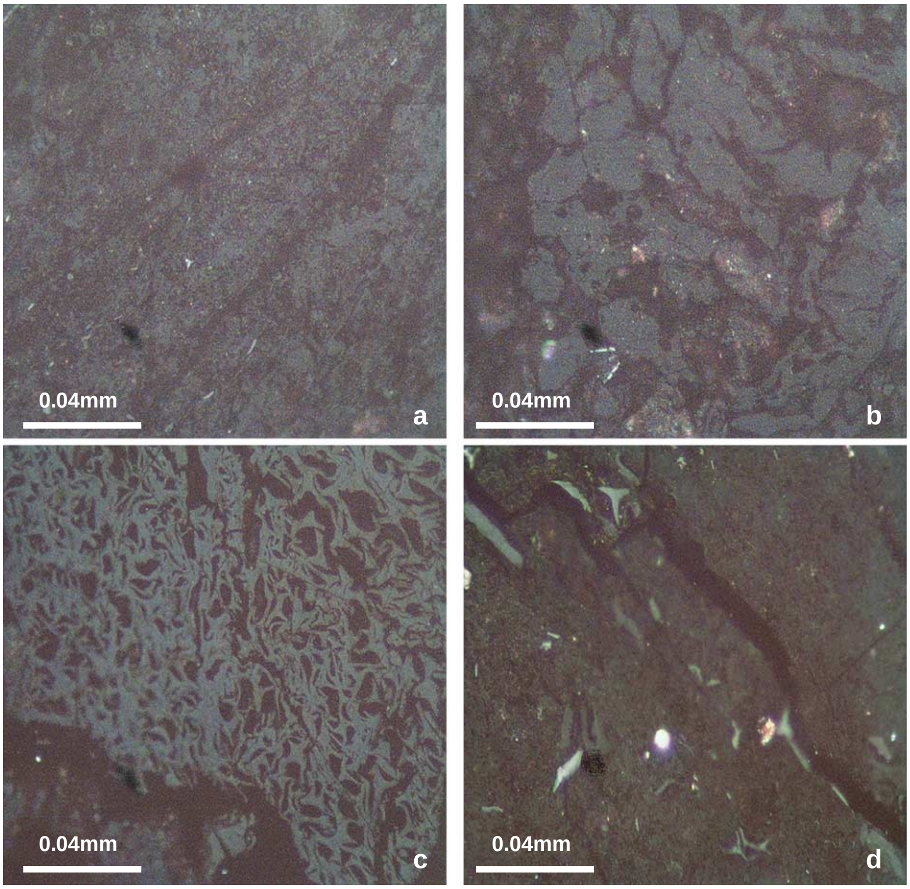

Fig. 6. Macerals of the vitrinite group in Shenglic coal: a) Vitrodetrinite in MY-12; b) Corpcollinite in MY-12; c) telinite in MY-2; d) Desmocollinite in MY-7.

The top section of the coal seam (MY-2, MY-3) is characterized by a low-lying marsh with relatively oxidizing open water body and higher detrital influence.

3.4. Geochemistry

Table 4 summarizes the major and trace element concentrations in the coal samples from coal seam #6-1. As for most coals, the inorganic fraction is clearly dominated by Si and Al minerals, followed by Ca, S and Fe bearing species. However, as previously stated, it should be pointed out that although high-Ca contents were determined in some samples (up to 4.7% db), calcite is not present (in XRD detectable amounts). Dolomite is detected at trace levels by XRD analysis in some samples from the upper section. The Ca/Mg ratio (close to 9 in most samples) is too high to infer that Ca is present in dolomite. Consequently other modes of occurrence for Ca, such as organic affinity (including the traces of weddellite or other common Na, Mg, Sr or Mn oxalates), have to account for most of the Ca occurrence in the top section of this coal.

As, Be, Cs, Ge, Hg, Sb, U, and W are highly enriched in the coal samples when compared with worldwide coal concentrations (Swaine, 1990).

- Ge, with a bulk coal mean concentration of 427 μg/g (22–1894 μg/g) is clearly enriched when compared with the usual content in coal: 0.5–50 μg/g. For US coal samples, a mean of 5.7 μg/g was reported (Dr. R.B. Finkelman, pers. com.). The highest Ge content (MY-7 and MY-9 with 1894 and 1116 μg/g, respectively) is found in samples

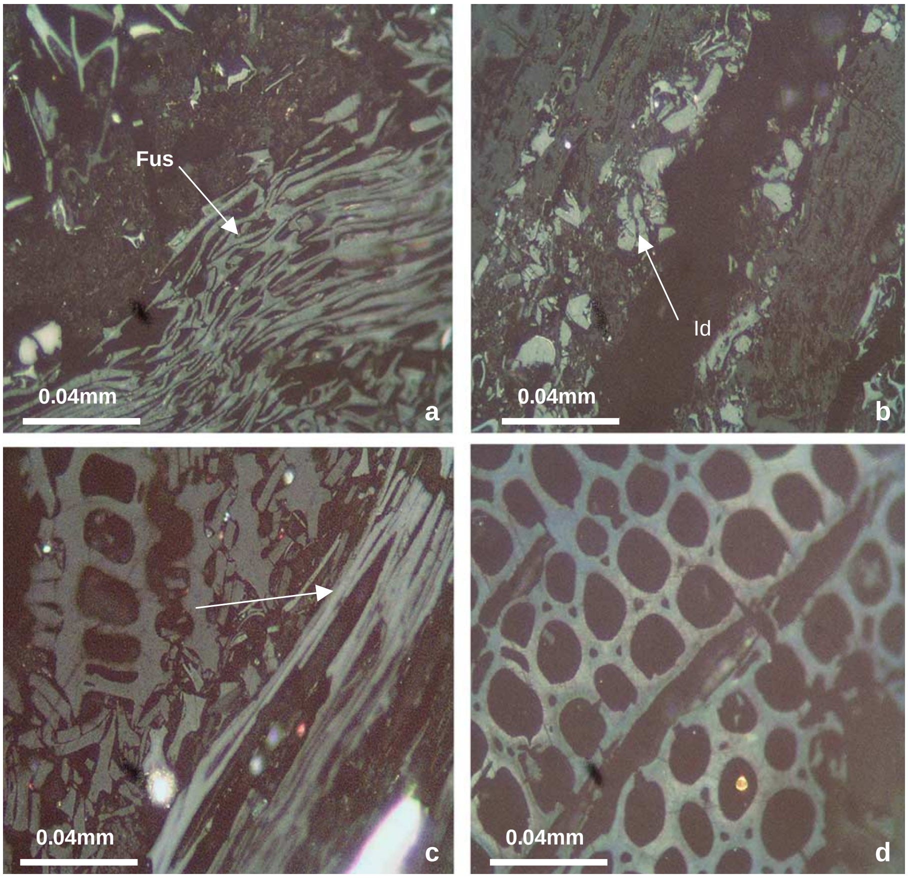

Fig. 7. Macerals of the inertinite group in Shengli coal: a) Fusinite in MY-7; b) Inertodetrinite in MY-8; c) Semifusinite in MY-14; d) Fusinite in MY-3.

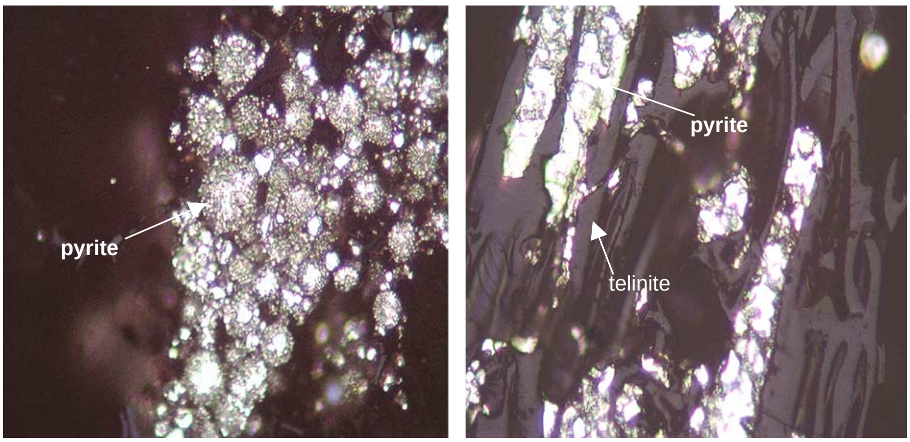

Fig. 8. Pyrite occurrence in Shengli coal: left: framboidal pyrite in MY-8 coal sample, right: block crystalline pyrite in telinite in MY-14 coal sample.

Table 4
Major and trace element concentrations in the coal samples from coal seam #6-1 from Wulantuga mine in the Shengli coal field

wt.%	MY-2	MY-3	MY-4	MY-5	MY-6	MY-7	MY-8	MY-9	MY-10	MY-11	MY-12	MY-14	Mean	Worldwide range	
	Top											Bottom		Max	Min
HTA	32	29	34	19	14	15	16	5	17	39	12	29	22		
Si	14	13	15	7	5	7	3	<0.1	5	14	3	6	8		
Al	2.1	2.1	2.0	1.2	0.7	0.3	0.6	0.2	0.7	3.4	1.0	2.4	1.4		
Ca	4.6	4.7	3.8	3.5	3.1	3.6	0.6	0.4	0.5	0.5	0.5	0.4	2.2		
K	0.1	0.1	0.3	0.1	<0.1	0.1	<0.1	<0.1	0.1	0.5	<0.1	0.2	0.1		
Na	0.2	0.2	0.1	0.2	0.2	0.2	0.1	0.1	0.1	0.1	0.1	0.1	0.1		
Fe	1.4	0.7	0.7	0.5	0.5	0.9	1.4	1.0	1.5	1.9	0.8	2.2	1.1		
S	0.2	0.3	0.3	0.3	0.3	0.5	1.8	1.5	2.0	1.9	1.1	2.5	1.0		
Mg	0.6	0.6	0.6	0.7	0.6	0.6	0.2	0.2	0.2	0.4	0.2	0.3	0.4		
μg/g															
Hg	18	25	2	0.9	0.4	3.2	0.7	0.4	1.5	0.2	0.2	0.03	4	1	0.02
Li	19	18	16	7	4	2	3	0.1	4	24	8	16	10	80	1
Be	85	77	58	38	2	10	28	12	17	15	19	17	33	15	0.1
B	21	17	16	31	70	97	115	183	139	91	209	168	92	400	5
P	95	40	36	12	16	7	10	8	14	44	18	42	28	3000	10
Sc	2	2	3	1	1	<0.1	<0.1	<0.1	1	3	2	5	2	10	1
Ti	1214	1137	1712	620	393	327	232	67	404	1143	147	555	674	2000	10
V	37	25	26	11	7	4	3	1	8	33	10	40	17	100	2
Cr	17	14	18	7	6	3	4	3	6	20	10	25	11	60	1
Mn	70	119	88	58	38	23	10	10	15	29	15	27	43	300	5
Co	11	12	8	5	3	2	1	2	3	4	11	11	6.	30	1
Ni	63	75	36	11	5	5	2	3	3	6	5	8	18	50	1
Cu	20	19	19	7	5	7	4	8	12	22	5	18	12	50	1
Zn	156	183	101	37	12	9	4	139	18	17	8	33	54	300	5
Ga	8	8	7	2	2	1	1	1	2	8	2	7	4	20	1
Ge	176	106	22	59	391	1894	422	1116	418	146	696	210	427	50	1
As	407	25	16	9	10	17	546	718	573	368	511	1321	356	80	1
Se	14	13	11	9	1	<0.1	<0.1	<0.1	<0.1	<0.1	<0.1	<0.1	4	10	0.1
Rb	7	8	19	6	2	3	1	1	5	46	4	21	10	50	2
Sr	562	622	504	438	361	369	63	51	57	58	53	50	273	500	15
Y	18	8	7	4	3	4	2	2	4	8	9	17	7	50	2
Zr	80	57	52	22	15	10	8	2	13	54	15	45	31	200	5
Nb	5	3	5	2	2	1	1	<0.1	1	3	1	2	2	20	1
Mo	2	1	<0.1	<0.1	14	14	<0.1	1	<0.1	<0.1	<0.1	<0.1	3	10	0.1
Cd	1.0	0.9	0.3	0.1	0.1	<0.1	<0.1	<0.1	<0.1	0.1	<0.1	0.3	0.2	3	0.1
Sn	<0.1	<0.1	<0.1	<0.1	<0.1	<0.1	<0.1	<0.1	<0.1	1	<0.1	<0.1	0.2	10	1
Sb	177	314	98	83	40	94	15	38	15	5	21	5.3	75	10	0.1
Cs	8	6	9	3	2	2	3	3	5	32	9	34	9	5	0.1
Ba	296	414	331	184	113	127	61	52	81	137	77	79	165	1000	20
Hf	1.8	1.3	1.3	0.6	0.4	0.2	0.2	0.1	0.3	1.4	0.5	1.0	0.8	5	1
Ta	0.4	0.3	0.4	0.2	0.3	0.1	<0.1	<0.1	0.1	0.3	0.1	0.2	0.2	2	0.1
W	534	911	383	495	428	721	328	178	411	261	707	617	507	5	1
Tl	3.1	4.1	5.0	5.5	4.4	1.9	1.1	0.4	1.5	0.5	0.1	0.2	3	1	0.1
Pb	9	6	7	4	4	2	2	1	4	10	4	7	5	80	2
Bi	<0.1	<0.1	<0.1	<0.1	<0.1	<0.1	<0.1	<0.1	<0.1	0.2	<0.1	<0.1	<0.1	1.0	0.1
Th	2	2	3	1	1	1	1	<0.1	1	3	1	3	2	10	1
U	105	43	26	19	2	1	0.3	0.2	0.4	1	0.9	2	17	10	1
ng/g															
Ir	51	29	10	13	<10	<10	<10	<10	<10	<10	<10	<10	<10	<10	<10
Pt	<10	<10	<10	<10	<10	<10	<10	<10	<10	<10	<10	<10	<10	<10	<10
Au	26	<10	<10	<10	<10	11	<10	<10	<10	<10	<10	<10	<10	<10	<10

Table 4 *(continued)*

wt.%	MY-2	MY-3	MY-4	MY-5	MY-6	MY-7	MY-8	MY-9	MY-10	MY-11	MY-12	MY-14	Mean	Worldwide range	
	Top											Bottom		Max	Min
La	19.51	11.56	10.69	5.45	4.75	3.60	2.78	1.15	4.32	9.51	4.13	12.56	7.55	40	1
Ce	33.57	19.63	19.15	10.09	8.11	6.97	5.14	2.27	8.40	18.33	9.01	27.94	14.1	70	2
Pr	4.00	2.25	2.24	1.16	0.90	0.85	0.59	0.30	1.03	2.31	1.23	3.26	1.7	10	1
Nd	17.22	9.09	8.70	4.54	3.48	3.61	2.37	1.38	4.49	9.42	5.97	14.32	7.1	30	3
Sm	2.56	1.22	1.23	0.69	0.47	0.57	0.32	0.23	0.67	1.48	1.21	2.35	1.1	6	1
Eu	0.45	0.27	0.26	0.14	0.10	0.13	0.07	0.05	0.15	0.30	0.28	0.53	0.2	2	0.1
Gd	3.10	1.52	1.44	0.81	0.62	0.76	0.39	0.28	0.87	1.69	1.55	3.09	1.3	4	0.1
Tb	0.44	0.21	0.20	0.11	0.08	0.11	0.05	0.04	0.12	0.24	0.25	0.49	0.2	1	0.1
Dy	2.62	1.21	1.21	0.66	0.50	0.69	0.28	0.23	0.72	1.41	1.55	3.03	1.2	4	1
Ho	0.53	0.23	0.23	0.12	0.09	0.13	0.05	0.04	0.13	0.27	0.32	0.61	0.2	2	0.1
Er	1.44	0.60	0.63	0.34	0.25	0.37	0.14	0.13	0.35	0.72	0.85	1.64	0.6	3	1
Tm	0.26	0.09	0.11	0.06	0.04	0.06	0.02	0.02	0.06	0.13	0.15	0.28	0.1	1	0.1
Yb	1.51	0.55	0.69	0.35	0.26	0.36	0.16	0.11	0.31	0.78	0.86	1.62	0.6	3	0.1
Lu	0.27	0.10	0.11	0.06	0.04	0.06	0.02	0.02	0.05	0.13	0.14	0.27	0.1	1	0.1

Values in wt.% or ug/g on dry coal basis.

from the central section of the seam without any definite trend or correlation with other elements. The markedly negative correlation of the Ge content with the ash yield and the group of elements associated with Al–Si minerals ($r = -0.6$ for correlation with most of these elements) points to the association of Ge with organic matter.

- As, with a mean concentration of 356 μg/g (9–1321 μg/g), is also highly enriched when compared with worldwide coal concentrations: 0.5–80 μg/g. For US coal samples, a mean of 24 μg/g was reported (Dr. R.B. Finkelman, pers. com.). The lower coal section is clearly enriched (368 to 1321 μg/g) with respect to the upper part (9 to 25 μg/g), with the exception of the top sample (MY-2, 407 μg/g). The high association of As with Fe and S ($r = 0.7$ and 0.8) points to a sulfide/arsenide mode occurrence, at least in the lower coal section.
- W, with a mean concentration of 501 μg/g (178 to 911 μg/g) is strongly enriched when compared with usual worldwide coal concentrations: 0.5–5 μg/g. For US coal samples, a mean of 1 μg/g was reported (Dr. R.B. Finkelman, pers. com.). Peak W concentrations are identified sporadically along the whole coal section probably associated with the organic matter (as inferred from preliminary density fractionation studies) and with local accumulation of scheelite rich partings. W contents are only moderately correlated with Co and Sb ($r = 0.5$–0.6).
- Hg, with a mean concentration of 4.3 μg/g (0.03–25 μg/g), is also highly enriched when compared with worldwide coal concentrations: 0.02–1.0 μg/g. For US coal samples, a mean of 0.17 μg/g was reported (Dr. R.B. Finkelman, pers. com.). The highest Hg contents are located in the top part of the coal seam (18–24 μg/g for MY-2 and MY-3, and 0.03–3.2 μg/g for the middle and lower sections). An evident correlation ($r = 0.85$–0.95) of Hg with Ca, Sb, Ni, Zn, Se, Cd and Co for the 6 top samples enriched in most of these elements is probably due their common diagenetic origin.
- Sb, with a mean concentration of 75 μg/g (5 to 314 μg/g) is clearly enriched when compared with worldwide coal concentrations: 0.1–10 μg/g. For US coal samples, a mean of 1.2 μg/g was reported (Dr. R.B. Finkelman, pers. com.).The highest Sb contents are located in the upper part of the coal seam (40–314 and 5–38 μg/g for the upper and lower sections), with an evident correlation ($r = 0.7$–0.8) with Ni, Zn, Cd, Hg and Co.
- U, with a mean concentration of 17 μg/g (0.2 to 105 μg/g), is enriched when compared with worldwide coal concentrations: 0.5–10 μg/g. For US coal samples, a mean of 2.1 μg/g was reported (Dr. R.B. Finkelman, pers. com.). The highest U contents are also found in the top (19–105 and 0.2–2.0 μg/g for the top and middle-bottom samples). A high correlationship was found for Be, P, Se, Cd ($r = 0.8$) and

Zr, LREE, Hf ($r = 0.7$). A negative correlationship was determined with Ge and B.

- Cs, with a mean concentration of 9 μg/g (2 to 34 μg/g), is enriched when compared with worldwide coal concentrations: 0.1–5 μg/g. For US coal samples, a mean of 1.1 μg/g was reported (Dr. R.B. Finkelman, pers. com.). Cs contents are highly correlated with the Al–Si associated group of elements (Cr, Sc, Rb, Al, K, V, Th, $r = 0.8$–0.7) and show a trend to decrease in the middle section of the seam as the above Al–Si elements.
- Be, with a mean concentration of 33 μg/g (10 to 85 μg/g), is enriched when compared with worldwide coal concentrations: 0.1–15 μg/g. For US coal samples, a mean of 2.2 μg/g was reported (Dr. R.B. Finkelman, pers. com.). Be contents are highly enriched in the top section (38–85 and 10–28 μg/g for the top and bottom samples) and consequently highly correlated with Mn, Ni, Se, Sr, Zn, Cd, Ba and U, ($r = > 0.8$).
- Platinum group elements (PGE): only Ir was detectable, with a mean concentration of 26 ng/g (10 to 51 ng/g), which is in the range of the usual concentrations when compared with the few coal concentrations available worldwide (<50 ng/g, Swaine, 1990).
- Au, with a mean concentration of 18 ng/g (11 to 26 ng/g). Given that concentrations of up to 10 ppb could be expected in most coals (Swaine, 1990), the contents found in this study could be considered in the usual rage. Ir and Au are present in detectable levels in the upper section samples, as described for Ca, Cd, Hg, Sb, Se, Ni, and Zn.

The other elements analyzed are present in the usual concentration ranges in coal, most of them in relatively low levels.

Germanium in coal is frequently present with an organic affinity (Finkelman, 1982). This element tends to be concentrated in the bottom and/or top of the coal seam. According to Yudovich (2003), Zilbermints et al. (1936) first noted Ge-enrichment near the roof, floor, and partings of Donetsk basin coals. Pavlov (1966), defined this phenomenon as the ‘‘Zilbermints Law’’ in honor of the first observer. According to Yudovich (2003) the ‘‘Zilbermints Law’’ has been observed in most geochemical studies of coal (see as examples Breger and Schopf, 1955; Admakin, 1970; Kulinenko, 1976; Eskenazy, 1996; Hower et al., 2002), but this is not the case of this study. However model 3 for Ge enrichment (Yudovich, 2003) is described for coal seams with similar lithology at the top and bottom, and without vertical trends in ash yields or maceral contents, but with a parting splitting the coal. In such a case, one may find additional intra-bed Ge-enriched zones near the parting. The thicker the parting, the thicker is the Ge-enriched zones. The enrichment above the parting is often greater than beneath the parting. Greb et al. (2002) reported for multiple-bench architecture in coal that partings represent a new start to the mire. Consequently, it should be possible that Ge contents increases around these seam units. Furthermore, an irregular Ge distribution in the coal seam can be found if the coal seam contains benches composed of low-ash vitrain with an enhanced Ge-content (model 4), or if the coal seam is thick and made up of agglomerations of multiple distinct depositional environments, sometimes separated by partings.

In high Ge coal basins, thin coal seams have generally a higher Ge content than the thick ones (Hower et al., 2002). Ge enters the peat by way of the roof and floor rocks, and therefore thin coals dominated by ‘‘margins’’ have the highest probabilities to be enriched in this element (Kulinenko, 1976; Hower et al., 2002).

Germanium in coal may have a variety of sources (Hower et al., 2002). Zhuang et al. (1998) attributed high Ge concentration in a Chinese coal to the syngenetic adsorption and complexation by humic acids. Hydrothermal and volcanic activity was the cause of very high Ge contents in different coals from Bulgaria and Russia (Eskenazy, 1996; Vassilev et al., 1996; Seredin and Danilcheva, 2001). Thus, both syngenetic and diagenetic trapping of Ge in coal are possible. In the later case, it is more probable that the element is enriched in the top and bottom of the coal seam.

The distribution of the mean Ge contents in coal seam #6-1 shows a fan-shaped decreased trend from the Southeast to the Northwest at the margin of the coal field (Fig. 2). The gradient of Ge content is very steep at the margin of the coal seam. On the other hand a major organic affinity is inferred for the occurrence of Ge. Probably these geochemical distribution patterns are the product of: a) the syn-sedimentary Ge trapping along the border of the basin, or b) a post-sedimentary trapping of Ge supplied by the weathering of presently eroded coal outcrops from the Southeastern border of the basin. Although, in this study we do not have complete information of the distribution of Ge content across the study area, neither about the possible post-sedimentary alterations, we suggest a major synsedimentary origin (in a context with high Ge source rocks) for the Ge anomaly found in the Shengli coal, based on the organic affinity and the above concentration gradient.

The elements analyzed may be classified in 3 groups according the vertical concentration trends identified in coal #6-1.

- S contents range from 0.2% to 2.5%, with a clear trend to increase in the lower section (1.1–2.5% db) with respect to the upper part (0.2–0.5% db). A similar trend was found for the profile concentration of pyrite, Fe and As, although relatively high contents of As and Fe were measured in top sample MY-2.
- An inverse concentration trend was identified for Ca, Na, Mg, Be, Mn, Ni, Se, Sr, Zn, Cd, Sb, Ba, Tl, Hg, and U (and also Au and Ir). Thus, the concentrations of Ca in the upper coal seam section are one order of magnitude higher with respect to the bottom part (3.1–4.6%db with respect 0.4–0.6%db).
- Finally, contents of Al, Si, K, P, Li, V, Cr, Sc, Ti, Cu, Ga, R, Y, Zr, Nb, REEs, Pb and Th are markedly depleted in the central section of the seam. Most of these elements are usually associated with clay minerals or Al–Si detrital mineral assemblages.

The high S, Fe and As contents (group 1) in the lower part suggest a reduced marsh environment in the lower part of the coal seam. This environment evolves towards a more oxidizing marsh environment in the upper part of the coal seam with the consequent enrichment in Ca, Mg, Na, Sr, Mn and Ba. However, the very high As content is probably the result of a high-As geochemical anomaly in the source area of the basin.

The higher contents of group 3 elements (as well as of ash yields) in the top and bottom of the coal seam could be attributed to a possible evolution from a high water table low-lying marsh environment to a raised marsh into an low-lying marsh, with a open water body and higher detrital influence at the top of the seam. The isolated enrichment of Fe and As in the top sample of the coal seam could be related to diagenetic process.

The origin of the markedly high content of the group 2 elements in the top coal section should be pointed out. As stated above, Ca, Na, Mg, and Mn (and probably Sr and Ba) are enriched because of the formation of oxalates in the top section due to leaching of coal with high $Ca(OH)_2$ hydrothermal solutions or to a syngenetic formation of such unusual organic minerals. The high association of Ni, Be, Se, Zn, Cd, Sb, Tl, Hg, and U (and also Au and Ir) with these oxalate-bearing coal samples may indicate an epigenetic alteration of the coal with enrichment of these trace elements. Especially noticeable are the very high Sb and Hg contents. However, Kalaitzidis and Christanis (2002) found oxalates in a high As, Se, Br and U peat deposit. Consequently, although we are in favor of the the epigenetic alteration, the origin of this organic mineralization and trace metals enrichment in the top of the coal seam could be both syngenetic and/or epigenetic. Nevertheless, the high enrichment in this large number of elements demands a high metal geochemical anomaly in the source area. Thus, it should be pointed out that the coal basin is surrounded (West and Northwest) by Quaternary basalts and diorite granites from the Mesozoic. The occurrence in Shengli coal of detrital W-bearing minerals, usually formed in mineralized veins in granites (scheelite), is consistent with the existence of a high metaliferous source area. Furthermore, granite intrusions on Permian limestone bodies are present in the zone, which could account for the high contents of diverse metals in the Shangli coal.

Seredin (2004) reported the general characteristics of the high epigenetic mineralization of the Au–Pt group elements (PGE) at the high-Ge Cenozoic brown coal deposit of Pavlovsk (Primorye, Russia). This author defined the geochemical patterns of this deposit as: ‘The germanium-bearing coal beds at the Pavlovsk deposit are enriched with As, Sb, W, Mo, Be, U, and Cs’. Furthermore, high Hg contents have been found at the Pavlovsk deposit. Identical geochemical patterns were found at the high Ge Shengli coal deposit with the exception of Mo. According to Seredin (2004), the precious metal mineralization at the Pavlovsk deposit is polygenic and polychronic. This was formed by the fluid-hydrothermal activity related to two impulses of a rift-genetic Late Cenozoic volcanism. Metals are also enriched in the top section of coal seam due to the influence of hydrothermal fluids migrating into sandstone bodies at the top of the coal strata. The probable sources of the ore components could be magmatic chambers and the Early Cambrian carbonaceous shales. The latter contain Au–PGE mineralization in the neighboring area in China (Lott et al., 1999). One of the mineralization stages is associated with the Quaternary volcanism also present in the Shengli coal deposit. It is worth noting that Pavlovsk and Shengli coal deposits are located around 1000 km apart.

Seredin (2004) also stated that the ore deposit was discovered because 'In 1992, micrograins of gold were distinguished with an electron microscope in coals from the Luzanovsk depression'. Au micro-grains were also detected by SEM-EDX in this study. Consequently, an intensive geochemical exploration of Shengli coal filed is suggested.

In our opinion the enrichment of group 2 elements at the top section of the coal seam from Shengli coal deposit could be caused by an epigenetic process, due to a direct alteration by hydrothermal fluids (causing also the formation of oxalates) and/or due to the epigenetic enrichment of these metals in the source rocks, the last also probably accounting for the high metal content fixed by the organic matter and sulfides in coal (both at the top and bottom).

4. Conclusions

1) The Cretaceous Shengli sub bituminous coal is characterized by a relatively high ash yield (21%) and by relatively low calorific value (5697 kcal/kg daf, equivalent to 23.85 MJ/kg)) and sulfur content (1% db). The volatile matter yields and N contents in the upper section of the coal seam (MY-2 to MY-7) are relatively high, whereas calorific value and C, H and S exhibit a converse profile distribution. This could be due to a reduced marsh environment in the lower part of the coal seam.
2) Ge, As, W, Hg, Sb, U, Cs, and Be are highly enriched in the coal samples when compared with worldwide coal concentrations (Swaine, 1990) and US coals (Dr. R.B. Finkelman, pers. com.). with a mean concentration of 427 Ge μg/g (22–1894 μg/g), 356 As μg/g (9–1321 μg/g), 501 W μg/g (178 to 911 μg/g), 4.3 Hg μg/g (0.03–25 μg/g), 75 Sb μg/g (5 to 314 μg/g), 17 U μg/g (0.2 to 105 μg/g), 9 Cs μg/g (2 to 34 μg/g) and 33 Be μg/g (10 to 85 μg/g), respectively. A high metal geochemical anomaly from Quaternary basalts (West and Northwest) and the Mesozoic diorite granites in the source area may account for the high enrichment of this large number of elements.
3) The major mineral constituents of the coal samples are quartz (15%), kaolinite (4–5%), illite (1%), pyrite (<1%), feldspars (<1%), gypsum (weathering product, <2%) and traces of chlorite. Rare traces of scheelite ($CaWO_4$) and weddellite (an oxalate, $CaC_2O_4{\cdot}2H_2O$) were also detected by XRD and SEM.
4) The elements analyzed may be classified in three groups according to the vertical concentration trends identified in coal #6-1: a) S, Fe and As with a marked tendency to increase in the lower section; b) Ca, Na, Mg, Be, Mn, Ni, Se, Sr, Zn, Cd, Sb, Ba, Tl, Hg and U (and also Au and Ir) with an inverse concentration trend; and c) Al, Si, K, P, Li, V, Cr, Sc, Ti, Cu, Ga, R, Y, Zr, Nb, REEs, Pb and Th with lower contents in the central section of the seam. This geochemical pattern suggest: 1) a reduced marsh environment in the lower part of the coal seam which evolves towards a more oxidizing marsh environment in the upper part of the coal seam; and 2) a possible evolution from a high water table low-lying marsh environment to a raised marsh into an open water body low-lying marsh with a higher detrital influence at the top of the seam.
5) Although elements such as Ge, W and As are fixed syngenetically (at least partially) by the organic matter (Ge and W) and sulfides (As), in our opinion the enrichment of Be, Ni, Se, Zn, Cd, Sb, Tl, Hg and U (and also Au and Ir) at the top section of the coal seam from Shengli coal deposit could be caused by an epigenetic process, due to a direct alteration by hydrothermal fluids (also causing the formation of oxalates) and/or due to the epigenetic enrichment of these metals in the source rocks. The last also probably causing the high metal content fixed by the organic matter and sulfides in coal (both at the top and bottom).

An intensive geochemical exploration of Shengli coal filed is suggested since a coal deposit (Pavlovsk) with similar geochemical patterns contains Au-PGE mineralizations.

Acknowledgement

The authors would like to express their gratitude to the Spanish Ministry of Foreign Affairs and the Department of Science and Technology from Hubei for supporting this study. We would like to thank Mr. J. Elvira, Mrs. S. Martinez, Mrs. S. Rico and Mrs. Cabañas for their help in the analytical tasks and to Drs. R.B. Finkelman, J.C. Hower, Artur Stankievicz and G. Eskenazy for their very valuable comments and suggestions.

References

Admakin, L.A., 1970. Relationship between ash and germanium content of coal and its genetic significance. Doklady Akademii Nauk SSSR 192, 1353–1355.

ASTM D-3286, 1996. Gross Calorific Value of Solid Fuel by the Isothermal-Jacket Bomb Calorimeter.

Bechtel, A., Gruber, W., Sachsenhofer, R.F., Gratzer, R., Lücke, A., Püttmann, W., 2003. Depositional environment of the Late Miocene Hausruck lignite (Alpine Foreland Basin): insights from petrography, organic geochemistry, and stable carbon isotopes. International Journal of Coal Geology 53, 153–180.

Bechtel, A., Markic, M., Sachsenhofer, R.F., Jelen, B., Gratzer, R., Lücke, A., Püttmann, W., 2004. Paleoenvironment of the upper Oligocene Trbovlje coal seam (Slovenia). International Journal of Coal Geology 57, 23–48.

Breger, I.A., Schopf, J.M., 1955. Germanium and uranium in coalified wood from upper Devonian black shale. Geochimica et Cosmochimica Acta 7, 287–293.

Chung, F.H., 1974. Quantitative interpretation of X-ray diffraction patterns of mixtures: I. Matrix flushing method for quantitative multicomponent analysis. Journal of Applied Crystallography 7, 519–525.

Eskenazy, G., 1996. Factors controlling the accumulation of trace elements in coal. Annuaire de l'Universite de Sofia St. Kliment Ohridski, Faculte de Geologie et Geographie. Livre 1. Geologie 89, 219–236.

Finkelman, R.B., 1982. Modes of occurrence of trace elements and minerals in coal: an analytical approach. In: Filby, R.H. (Ed.), Atomic and Nuclear Methods in Fossil Energy Research. Plenum, New York, pp. 141–149.

Gruber, W., Sachsenhofer, R.F., 2001. Coal deposition in the Noric Depression (Eastern Alps): raised and low-lying mires in Miocene pull-apart basins. International Journal of Coal Geology 48, 89–114.

Hower, J.C., Ruppert, L.F., Williams, D.A., 2002. Controls on boron and germanium distribution in the low-sulfur Amos coal bed, Western Kentucky coalfield, USA. International Journal of Coal Geology 53, 27–42.

ISO-562, 1974. Hard Coal and Coke—Determination of the Volatile Matter.

ISO-1171, 1976. Solid Mineral Fuels—Determination of Ash.

ISO-589, 1981. Hard Coal—Determination of the Total Moisture.

Kalaitzidis, S., Christanis, K., 2002. Mineral matter in the Philippi peat in relation to peat/lignite-forming conditions in Greece. Energy Sources 24, 69–81.

Kulinenko, O.R., 1976. Relationship between germanium content and seam thickness in Paleozoic coal basins of Ukraine. International Geology Review 19, 1182–1187.

Li, S., Li, B., Yang, S., Huang, J., Li, Z., 1984. Sedimentation and tectonic evolution of Mesozoic faulted coal basin in Northeastern China. Special Publication of the International Association of Sedimentologists 7, 387–406.

Li, S., Wu, C., Yang, S., Huang, J., 1988. Fault Basin Analysis and Coal Accumulation. Geological Publishing House, Beijing (in Chinese).

Lott, D.A., Coveney, R.M., Murowchick, J.B., Grauch, R.I., 1999. Sedimentary exhalative nickel–molybdenum ores in South China. Economic Geology 94, 1051–1066.

Pavlov, A.V., 1966. Composition of coal ash in some regions of the West Svalboard. Uchen. Zap. NIIGA [Proc Arctic Geology Sci.-resear. Inst.]. Regional Geology 8, 128–136.

Querol, X., Alastuey, A., Lopez-soler, A., Plana, F., Fernandez-Turiel, J.L.Rongsu, Zeng, Wendong, Xu, Xiguo, Zhuang, Spiro, B., 1997a. Geological controls on the mineral matter and trace elements of coals from the Fuxin basin, Liaoning Province, northeast China. International Journal of Coal Geology 34, 89–109.

Querol, X., Whateley, M.K.G., Fernandez-Turiel, J.L., Tuncali, E., 1997b. Geological controls on the mineralogy and geochemistry of the Beypazari lignite, central Anatolia, Turkey. International Journal of Coal Geology 33, 255–271.

Seredin, V.V., 2004. The Au–PGE mineralization at the Pavlovsk Brown Coal Deposit, Primorye. Geology of Ore Deposits 46 (1), 36–63.

Seredin, V.V., Danilcheva, J., 2001. Coal-hosted Ge deposits of the Russian Far East. In: Piestrzynski, A., et al., (Eds.), Mineral Deposits at the Beginning of the 21st Century. Swets and Zeitlinger Publishers, Lisse, The Netherlands, pp. 89–92.

Swaine, D.J., 1990. Trace Elements in Coal. Butterworth, London. 278 pp.

Vassilev, S.V., Eskenazy, G.M., Tarassov, M.P., Dimov, V.I., 1996. Mineralogy and geochemistry of a vitrain lens with unique trace element content from the Vulche Pole coal deposit, Bulgaria. Geologica Balcanica 25, 111–124.

Wang, Lanming, 1999. Introduction of the geological feature and explorating of Germanium deposit in Xilinguole League, Inner Mongolia. Inner Mongolia Geology 3, 16–21.

Wu, Wen, Mo, Ruoping, Wang, Zhimin, 2002. Occurrence features and geological work of Germanium resource in Yimin Coalfield, Inner Mongolia. Inner Mongolia Geology 1, 27–30.

Yudovich, Ya.E., 2003. Notes on the marginal enrichment of Germanium in coal beds. International Journal of Coal Geology 56, 223–232.

Zhuang, H., Lu, J., Fu, J., Liu, J., 1998. Lincang super-large germanium deposit in Yunnan province, China: sedimentation, diagenesis, hydrothermal process and mineralization. Journal of China University of Geosciences 9, 129–136.

Zilbermints, V.A., Rusanov, A.K., Kosrykin, V.M., 1936. On the question of Ge-presence in fossil coals. Acad. V.I. Vernadsky-k50-letiyu nauchnoi deyatel'nosti [Up to 50-Anniversary of his Science Activity], AN SSSR [Acad. Sci. USSR], Moscow, vol. 1, pp. 169–190.